# Validation and Material Modeling of Polymers by Employing MAT_SAMP-1

Kunio TAKEKOSHI and Kazukuni NIWA
*TERRABYTE Co., Ltd, 3-21-4, Yushima, Bunkyo-ku, Tokyo, 113-0034, Japan*

## Abstract

*We have developed a method to determine plastic Poisson's ratio and its corresponding stress – strain curves, where newly redefined true stress expression including elastic and plastic Poisson's ratios is employed. The plastic Poisson's ratio is used to predict permanent volumetric deformation which is one of the mechanical characters associated with crazing. Although the crazing is one of the most important issues to be tackled in analysis, methods to determine the plastic Poisson's ratio and its corresponding data have not been discussed sufficiently in previous papers. Thus we show and discuss how we determine and validate these data. Additionally, in order to complement the method, we provide two techniques to utilize MLYS (Multi-Linear Yield Surface) and to evaluate damage property. We show MLYS could make analysis incorporating isochoric plasticity in compressive state stable. Furthermore we show that these methods are valid and useful through the numerical results.*

*Keywords: SAMP-1, MLYS, Plastic Poisson's Ratio, Damage effect*

## Introduction

Since SAMP-1 (Semi-Analytical Model for Polymers with $C^1$ – differentiable yield surface [1]) was available from the release of LS-DYNA® version 971, many efforts have devoted to the establishment of methods for preparing and validating input data for this model [2-5]. Thanks to many techniques reported in previous papers, we think we have become accustomed to the utilization. However we also think there still remain several fields to be discussed further, the plastic Poisson's ratio and shape of the yield surface. We propose our methods for validation and material modeling of polymers, especially focusing on the two issues.

## SAMP-1

SAMP-1 was developed by S. Kolling *et al*. [1]. Its main project is 'to include all relevant experimentally observed effects in one model'. One of the characteristic features is to adopt quadratic yield surface as a function of pressure $p$,

$$f\left(p, \sigma_{\mathrm{vm}}, \varepsilon_{\mathrm{eq,p}}\right) = \sigma_{\mathrm{vm}}^2 - A_0 - A_1 p - A_2 p^2 \leq 0. \quad (1)$$

Here, $\sigma_{\mathrm{vm}}$ is von Mises stress, $\varepsilon_{\mathrm{eq,p}}$ is equivalent plastic strain, $A_0, A_1, A_2$ are computed by three independent test results such as tension, compression and shear tests. Second characteristic feature is capable of realizing non-isochoric plasticity with non-associated flow rule. The expression of its plastic potential $g$ is

$$g(p, \sigma_{\mathrm{vm}}, \varepsilon_{\mathrm{eq,p}}) = \sqrt{\sigma_{\mathrm{vm}}^2 + \alpha p^2}\,, \qquad \alpha = \frac{9}{2}\frac{1-2\nu_{\mathrm{p}}}{1+\nu_{\mathrm{p}}} \tag{2}$$

, where $\nu_{\mathrm{p}}$ is the plastic Poisson's ratio. It is defined as the ratio of incremental plastic strains $\dot{\varepsilon}_{\mathrm{p,x}}, \dot{\varepsilon}_{\mathrm{p,y}}, \dot{\varepsilon}_{\mathrm{p,z}}$ and is not constant but variable as a function of equivalent plastic strain in SAMP-1. This is expressed as

$$\nu_{\mathrm{p}} \equiv -\frac{\dot{\varepsilon}_{\mathrm{p,y}}}{\dot{\varepsilon}_{\mathrm{p,x}}} = -\frac{\dot{\varepsilon}_{\mathrm{p,z}}}{\dot{\varepsilon}_{\mathrm{p,x}}} = \nu_{\mathrm{p}}(\varepsilon_{\mathrm{eq,p}}). \tag{3}$$

Damage model is also one of the attractive features, considering softening of Young's modulus and approximately predicting unloading displacement.

## Experiment

From the review, we easily find many experiments must be performed for the modeling. Preparations of curve data tabulated in Table 1 will be discussed.

In our method, material tests listed in Table 2 are usually employed under JIS (Japanese Industrial Standards). Here the definition of APR (Apparent Poisson's Ratio) is identical that of the conventional Poisson's ratio. The ratio is able to be measured in large strain region with DICM (Digital Image Correlation Method) so that it can be available in validation of LCID-P.

Table 1: Definition of curve data in MAT_SAMP-1

| Curve Data | Description |
|---|---|
| LCID-T/C/S/B | SS (true stress – plastic strain)<br>for Tension/Compression/Shear/Biaxial tension |
| LCID-D | Damage parameter – equivalent plastic strain |
| LCID-P | Plastic Poisson's ratio – equivalent plastic strain |

Table 2: Static material tests used in our method

| Test | Specification | Mechanical Property |
|---|---|---|
| Tension | JIS K7113-2 | LD (Load – Displacement)<br>Nominal Stress – Strain<br>Unloading displacement |
| Tension | JIS K7113-2 with 3D-DICM | APR, LD |
| Compression | JIS K7181 | LD |
| Shear | JIS K7214 with modified specimen | LD |
| Bending | JIS K7139A | LD, Unloading displacement |

# Modeling Method

## Plastic Poisson's Ratio and Its Corresponding Stress – Strain Relations

Among input data in Table 1, LCID-P significantly affects the cost of the preparation process. The reason for this is quite simple: modification of LCID-P as well as SS affects LD results. For example in tensile tests, cross sectional area of specimens depends on elastic and plastic Poisson's ratios. That is, if LCID-P is modified, SS relations also must be modified to reproduce LD relations. Thus simultaneous modification of several data is necessary in the modeling, but this generally causes confusion.

It should be noted that the example means true stress cannot be evaluated before the determination of LCID-P. Since we cannot measure/evaluate plastic strains, we must assume the ratio by trial-and-error procedure.

To carry out the tasks efficiently, we have redefined true stress expression where elastic and plastic Poisson's ratios are included, and we have developed a method to determine LCID-P and its corresponding SS data separately with the equation. The equation for uniaxial deformations is defined as [6,7]:

$$\sigma_{\mathrm{u}} = \Sigma_{\mathrm{u}} \exp\left[2\int_0^{\varepsilon_{\mathrm{u,p}}} \left\{\nu_{\mathrm{p}}\left(\varepsilon_{\mathrm{eq,p}}\right) - \nu_{\mathrm{e}}\right\} \mathrm{d}\varepsilon'_{\mathrm{u,p}}\right] \tag{4a}$$

$$\Sigma_{\mathrm{u}} = \frac{P_{\mathrm{u}}}{S}\exp\left(2\nu_{\mathrm{e}}\varepsilon_{\mathrm{u,t}}\right). \tag{4b}$$

Here, $\nu_{\mathrm{e}}$ is the elastic Poisson's ratio. Subscripts "u", "p" and "t" represent uniaxial, plastic and total, respectively. The term $\sigma_{\mathrm{u}}$ is true stress, $\Sigma_{\mathrm{u}}$ is tentative true stress obtained on the assumption that $\nu_{\mathrm{p}} = \nu_{\mathrm{e}}$. The term $P_{\mathrm{u}}$ is the load measured during experiments, $S$ is the cross sectional area of specimens at initial state. By the same manner, we also have the equation for biaxial deformations shown below [7]

$$\sigma_{\mathrm{b}} = \Sigma_{\mathrm{b}} \exp\left[\int_0^{\varepsilon_{\mathrm{b,p}}} \left\{\mu_{\mathrm{p}}\left(\varepsilon_{\mathrm{eq,p}}\right) - \mu_{\mathrm{e}}\right\} \mathrm{d}\varepsilon'_{\mathrm{b,p}}\right] \tag{5a}$$

$$\Sigma_{\mathrm{b}} = \frac{P_{\mathrm{b}}}{S}\exp\left[\left(\mu_{\mathrm{e}} - 1\right)\varepsilon_{\mathrm{b,t}}\right] \tag{5b}$$

where subscript "b" represents biaxial state. The terms $\mu_{\mathrm{e}}$ and $\mu_{\mathrm{p}}\left(\varepsilon_{\mathrm{eq,p}}\right)$ are elastic and plastic biaxial Poisson's ratios, respectively. These ratios are rewritten by "uniaxial" ratios:

$$\mu_{\mathrm{e}} = 2\nu_{\mathrm{e}}/\left(1 - \nu_{\mathrm{e}}\right) \tag{6}$$

$$\mu_{\mathrm{p}} = 2\nu_{\mathrm{p}}/\left(1 - \nu_{\mathrm{p}}\right). \tag{7}$$

Next, we introduce relations between plastic and equivalent plastic strains so that we can redefine the plastic Poisson's ratio as a function of plastic strain. According to references [1,8], we have a following functional to get the relations:

$$\varepsilon_{\mathrm{x,p}}\left(\varepsilon_{\mathrm{eq,p}}, f(\nu_{\mathrm{p}})\right) = \int_0^{\varepsilon_{\mathrm{eq,p}}} \frac{\sigma_{\mathrm{vm}}}{g} f(\nu_{\mathrm{p}}) \mathrm{d}\varepsilon'_{\mathrm{eq,p}} \tag{8}$$

$$f(\nu_{\mathrm{p}}) \equiv \frac{3}{2(1+\nu_{\mathrm{p}})}, \qquad \text{for uniaxial deformation}$$
$$\equiv \frac{3(1-\nu_{\mathrm{p}})}{2(1+\nu_{\mathrm{p}})}, \qquad \text{for biaxial deformation}$$

Finally the number of variables used in the equations can be reduced to three, $P_{\mathrm{x}}$, $\varepsilon_{\mathrm{x,t}}$ and $\sigma_{\mathrm{x}}$, thus the equations can be expressed as the following general form, self-consistent equation:

$$\sigma_{\mathrm{x}} = h(P_{\mathrm{x}}, \varepsilon_{\mathrm{x,t}}, \sigma_{\mathrm{x}}), \qquad \mathrm{x} = \mathrm{u \text{ or } b}. \tag{9}$$

Since two variables $P_{\mathrm{x}}$, $\varepsilon_{\mathrm{x,t}}$ are observable, we are able to solve the equations with an iterative algorithm and get the corresponding SS for every trial-LCID-P from the tentative SS.

The method can be separated into two stages and summarized in Table 3 and Table 4. In the first stage, tentative SS are determined, while elastic and plastic Poisson's ratios are assumed to be the same. In the second stage, LCID-P is determined and its corresponding SS are converted from SS data in stage 1. We named this conversion ASSC (Automatic Stress – Strain Conversion) after ASSR (Automatic Stress – Strain Recalibration) [9]. This separated processes realized by the ASSC enable us to prepare the data efficiently and successfully.

Table 3: Procedure in stage 1, Determination of tentative SS

| | | |
|---|---|---|
| Stage 1 | Step 1 | Determine/Assume SS by eq.4b/5b from experimental results.<br>Elastic and plastic Poisson's ratios are set to be the same in this stage. |
| | Step 2 | Validation analysis |
| | Step 3 | Quality check<br>→ If the validation results pass certain quality, then go to stage 2.<br>Otherwise go to step 4. |
| | Step 4 | Modify SS and then go back to step 2. |

Table 4: Procedure in stage 2, Determination of LCID-P and its corresponding SS

| | | |
|---|---|---|
| Stage 2 | Step 1 | Assume LCID-P |
| | Step 2 | Convert the stage1-SS into the corresponding SS by eq.4a/5a. |
| | Step 3 | Validation analysis |
| | Step 4 | Quality check<br>→ If the validation results pass certain quality, finish determination.<br>Otherwise go to step 5. |
| | Step 5 | Modify LCID-P and then go back to step 2. |

**Yield Surface**

In order to maintain the convexity of SAMP-1 yield surface and to realize reduced biaxial strength which was incorporated in buckling simulation associated with crazing [10], the condition eq.10, defined by uniaxial tension and compression stresses depending on $\varepsilon_{\mathrm{eq,p}}$, must be satisfied. In our method, pure shear stress depending on equivalent plastic strain $\sigma_{\mathrm{shear}}(\varepsilon_{\mathrm{eq,p}})$ is initially generated with eq.11 and then modified within the constraint of the condition, finally converted to LCID-S.

$$\sigma_{\mathrm{shear}}(\varepsilon_{\mathrm{eq,p}}) \geq \sqrt{\frac{\sigma_{\mathrm{tension}}(\varepsilon_{\mathrm{eq,p}}) \cdot \sigma_{\mathrm{comp.}}(\varepsilon_{\mathrm{eq,p}})}{3}} \tag{10}$$

$$\sigma_{\mathrm{shear}}(\varepsilon_{\mathrm{eq,p}}) = (1+\chi)\sqrt{\frac{\sigma_{\mathrm{tension}}(\varepsilon_{\mathrm{eq,p}}) \cdot \sigma_{\mathrm{comp.}}(\varepsilon_{\mathrm{eq,p}})}{3}} \quad ,\chi \geq 0 \tag{11}$$

LCID-P for tension regime is usually set to predict APR, while that for compression regime is set to 0.5, because thermoplastics do not show volume increase under compression [10]. However, we have experienced this configuration sometimes makes elements unstable under compressive state. When we face the problem, we usually switch from SAMP-1 mode to MLYS (Multi Linear Yield Surface) mode [8,9]. The mode additionally requires LCID-B and RBCFAC, a ratio biaxial vs. uniaxial compressive stresses. In our current method, biaxial stress is computed with eq.12 from SAMP-1 yield surface in stage 1, and then converted to LCID-B with eq.5a in stage 2.

$$\sigma_{\mathrm{b}}(\varepsilon_{\mathrm{eq,p}}) = \frac{3A_0}{A_1 + \sqrt{A_1^2 + A_0(9 - 4A_2)}} \tag{12}$$

On the other hand RBCFAC is tentatively set to 1, that is, Mises yield surface is selected for compression regime. Thus when MLYS mode is activated in our method, the yield surface is defined by quasi-SAMP-1 in tension and shear regimes and by Mises in compression regime as shown in Figure 1.

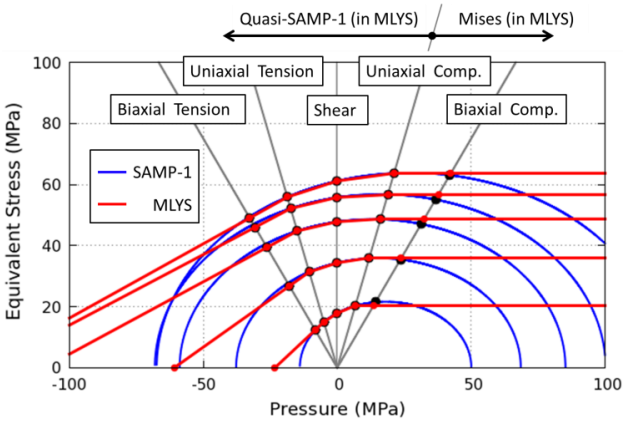


Figure 1: Comparison of the yield surfaces between SAMP-1 and MLYS modes.

### Damage

Hysteresis experiments were proposed to determine LCID-D [1]. However, unloading behaviors obtained in usual tests can also be used instead. For example, in tensile tests, unloading displacement at rupture point can be roughly estimated as illustrated in Figure 2. Furthermore, our method uses the following expression [4] to fit experimental results:

$$D(\varepsilon_{\mathrm{eq,p}}) = a\left[\exp(b\varepsilon_{\mathrm{eq,p}}) + \exp(c\varepsilon_{\mathrm{eq,p}})\right] \tag{13}$$

, where $a, b$ and $c$ are coefficients.

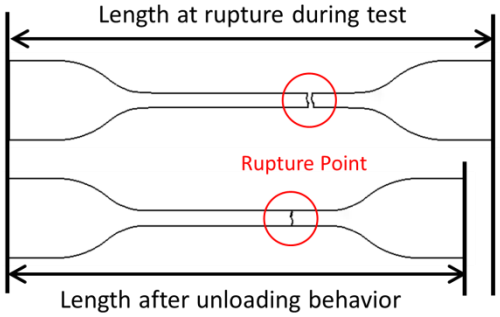


Figure 2: Estimation of unloading displacement at rupture point

## Material Modeling and Its Validation Results

Polycarbonate was chosen to verify our method, and material tests shown in Table 2 for this polymer have been carried out. Since polycarbonate is not a crystalline but an amorphous polymer, no anisotropic effects are expected. However we believe our technique is valid for crystalline thermoplastics such as Polypropylene.

### Plastic Poisson's Ratio and Its Corresponding SS (LCID-T)

Two kinds of tensile tests have been conducted. Figure 3 displays one of the experimental setups. We made an initial SS data in stage 1 by this measurement result, and its plastic strain was evaluated from the result by mechanical extensometer. Figure 4 sketches another setup to obtain APR and its sampling points A and B on the specimen.

In the first stage, we determined the tentative SS data on the assumption that both Poisson's ratios were set to 0.387. Figure 5 (Left) shows initial and final SS data determined in stage1, and Figure 5 (Right) provides the corresponding LD results. After some modifications, we achieved good SS quality.

In the second stage, we only adjusted the LCID-P, while "Final SS (stage1)" was fixed. Figure 6 (Left) depicts initial and final SS in stage 2 converted from "Final SS (stage1)" by the ASSC, Figure 6 (Right) shows a comparison between initial and final LCID-Ps. The LCID-P was initially set to 0.5, and then modified in subsequent iteration. Figure 7 shows validation results about APR and shows "final LCID-P" successfully predicted the experimental results. Furthermore, Figure 8 shows the reproducibility of the LD relations in both stages. Thus with the method, we were able to determine the two properties separately.

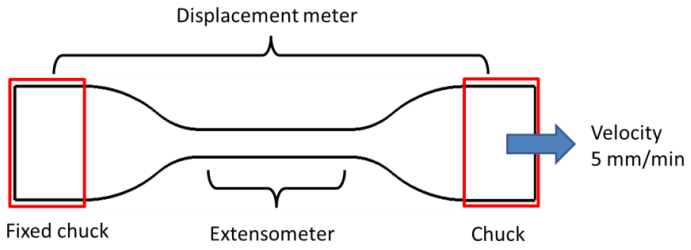


Figure 3: Tensile test with JIS K7113-2 specification

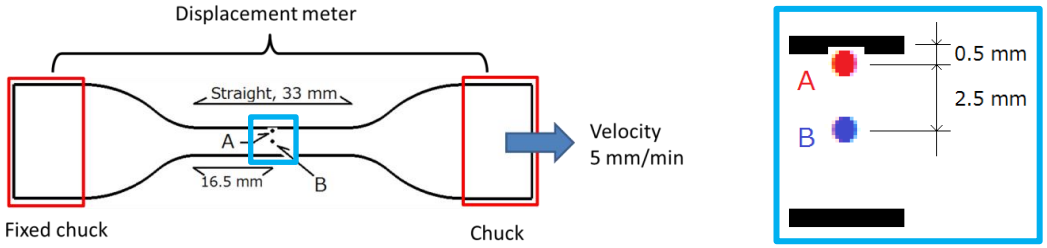


Figure 4: Tensile test setup and sampling points (A, B) of APR

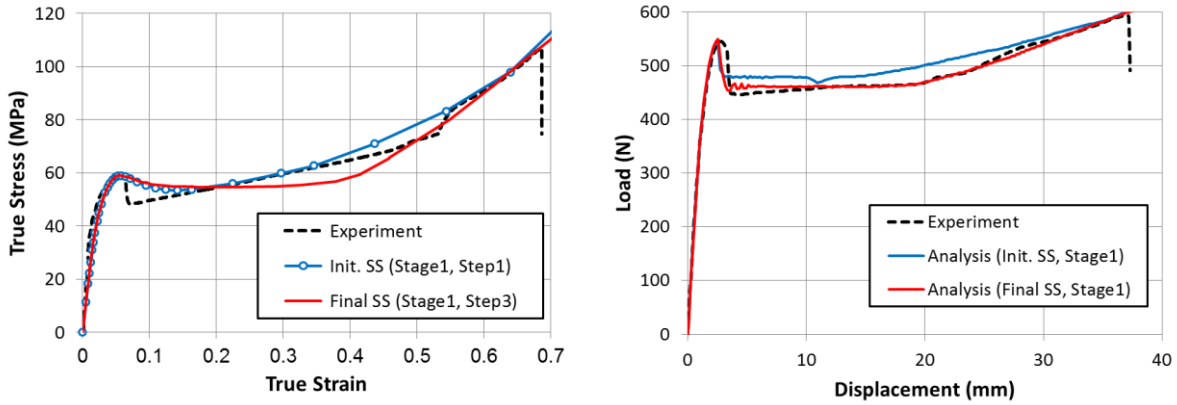


Figure 5: (Left) Comparison of true stress – strain relation in stage 1, (Right) Comparison of the corresponding LD results

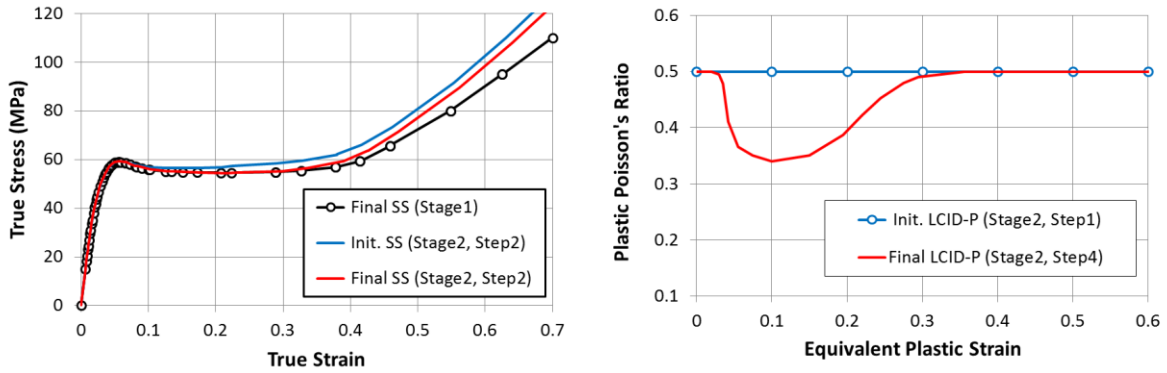


Figure 6: (Left) Comparison of true stress – strain relation in stage 2, (Right) Comparison of the LCID-P between initial and final steps

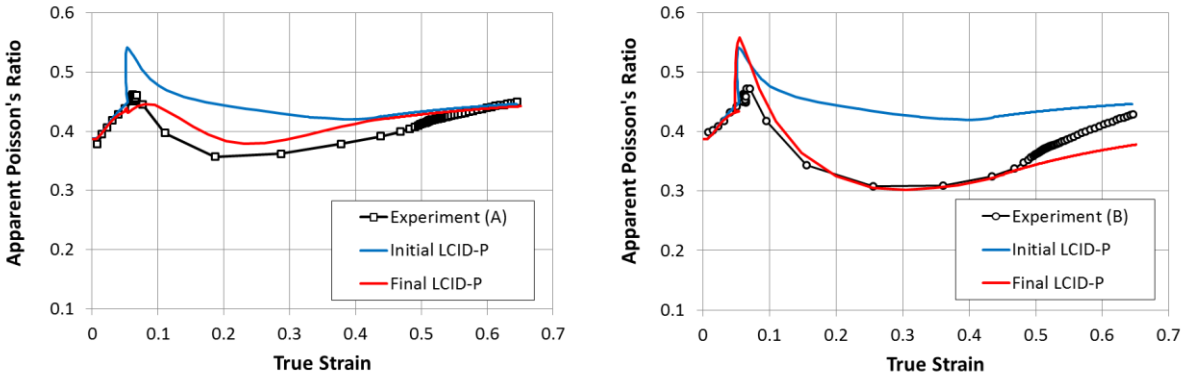


Figure 7: Validation results in terms of the APR

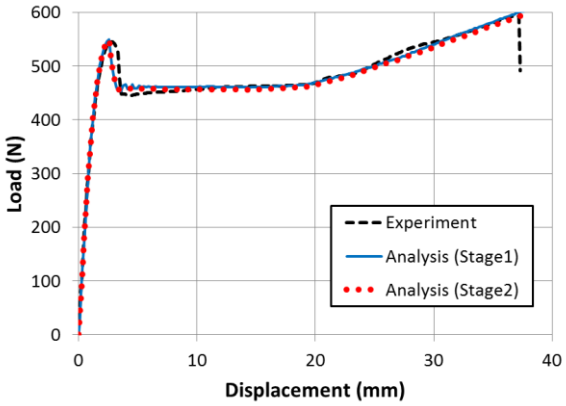


Figure 8: Comparison of the LD results

## Yield Surface

The LCID-S was modeled with eq.11 where $\chi$ was set to 0.025. The experimentally and computationally obtained the shear-LD relations exhibited qualitatively similar behavior.

The LCID-P in compression regime was modeled as isochoric. As mentioned above, analysis configured with SAMP-1 mode in combination with this LCID-P was suffered from instability in compression state. Figure 9 (Left) provides a result obtained in static compression analyses without erosion setup. Drastic reduction of compressive load was shown in SAMP-1 mode, indicating elements were unexpectedly deleted due to instability. On the contrary, with MLYS mode, the reduction did not appear and deformation of the specimen was reasonable in comparison with the experiment as shown in Figure 9 (Right).

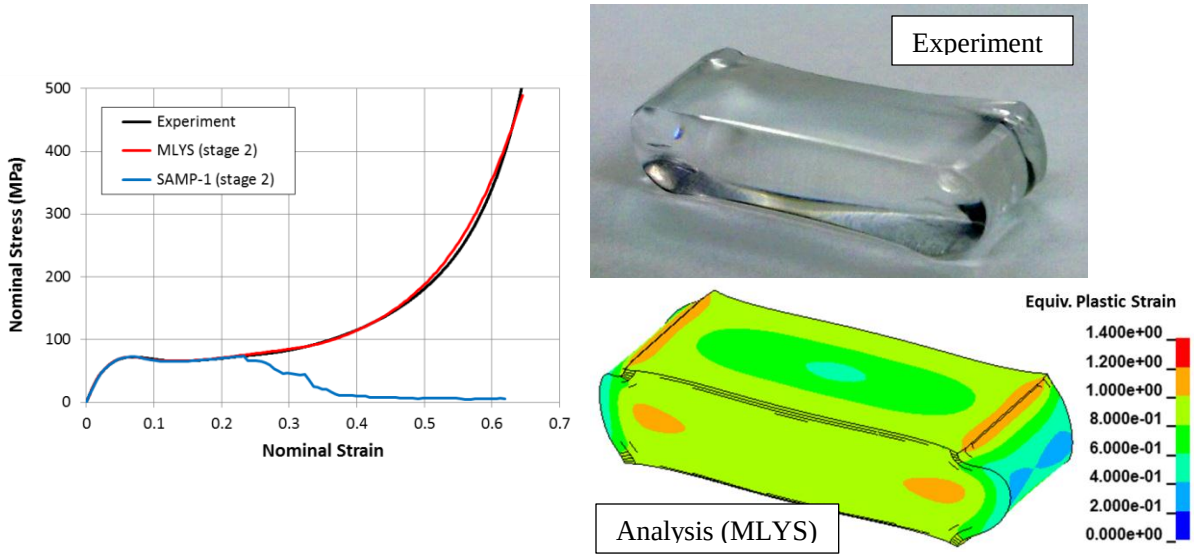


Figure 9: (Left) Nominal stress – strain relations in compression test (Right) Compressive deformation of the specimen

## Damage

We have fitted the LCID-D with eq.13 to predict the unloading displacement obtained in the tests listed in Table 2, and the parameters $a, b$ and $c$ were 0.6, 0.25 and -25.0, respectively. In the tensile test, it was estimated to be 8 mm. Figure 10 gives validation result with hysteresis analysis, where tension was applied to the specimen until the rupture point and then unloading was performed, showing expected unloading displacement 9 mm. In the bending test, specimens were not broken and showed significant unloading behavior from 17 to 5 mm in displacement. Figure 11 displays the result in the hysteresis bending test, where loading was performed until 17 mm and then unloading until 5 mm, showing the unloading behavior from 17 to 6 mm.

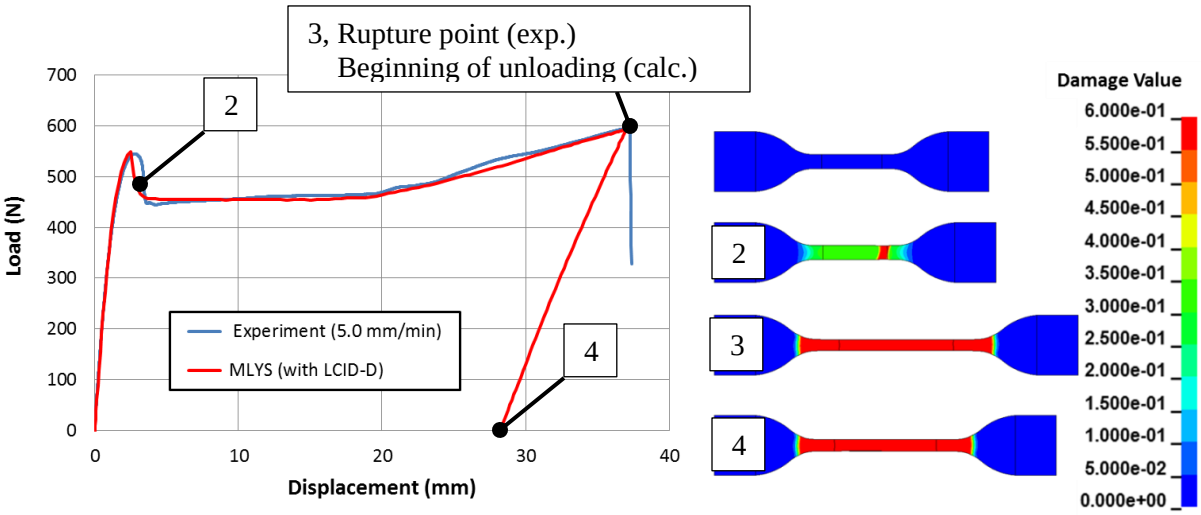


Figure 10: (Left) Validation result in the tensile test (Right) Accumulated damage plot

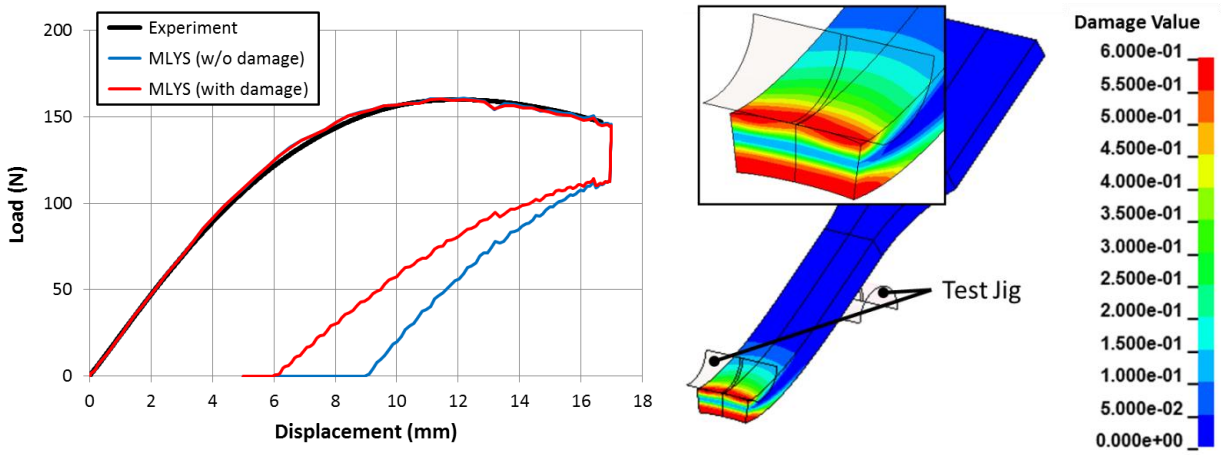


Figure 11: (Left) Validation result in the bending test (Right) Accumulated damage on the cross section of the specimen at maximum bending point

## Discussion

In the first example, we should address that although the initial SS in stage1 was made by approximately tracing experimental result, the corresponding simulation result was significantly different from the experimental LD data. We concluded this was because necking behavior was observed in the experiments and the measurement by the extensometer during the behavior was not reliable. There is room to modify the method.

For the modeling method of LCID-P and SS, we should discuss another method. Some papers have proposed effective method using 3D-DICM [2,4]. They measured full-field displacements and cross sectional area of specimens during tests, and then they evaluated true stress. This measurement is based on the following assumption: Stress distribution on the cross section is regarded as uniform. However, it is not always uniform as depicted in Figure 12. Moreover the different APR results in the inhomogeneous deformation as shown in Figure 7. Thus SS data created with this method should also be modified to predict experimental results. On the contrary, our initial tentative-SS was based on the extensometer and was less quality than their SS. Incorporating their technique will improve our method.

For the unstable calculation in compression analysis, we currently suspect that low multi-axial compression stress causes the problem. We found the curves LCID-C and LCID-T showed crossover at about 0.15 in equivalent plastic strain in stage 2, though the LCID-C was always larger than or equal to the LCID-T in stage 1 (Figure 13). This indicates that multi-axial compression state can be easily realized due to relatively small difference of pressure $\Delta p$ in SAMP-1 mode as illustrated in Figure 14. In fact, the triaxiality of the unstable elements started increasing after the crossover point and then oscillated between $10^2$ and $10^5$ just before deletion. This large triaxiality in SAMP-1 mode means the elements became so soft that element processing could not be performed. Hence, Setting RBCFAC to 1 prevents the appearance of quasi-triaxial compression state and is justified in terms of the calculation stability.

Finally let us discuss the way to determine the LCID-D. We used two experimental results to adjust the parameters, although the eq.13 has three coefficients. However, since damage quantity is not uniform on the cross section of the bending specimen as depicted in Figure 11, we believe the amount of the data to be fitted were sufficient and the LCID-D had been fitted.

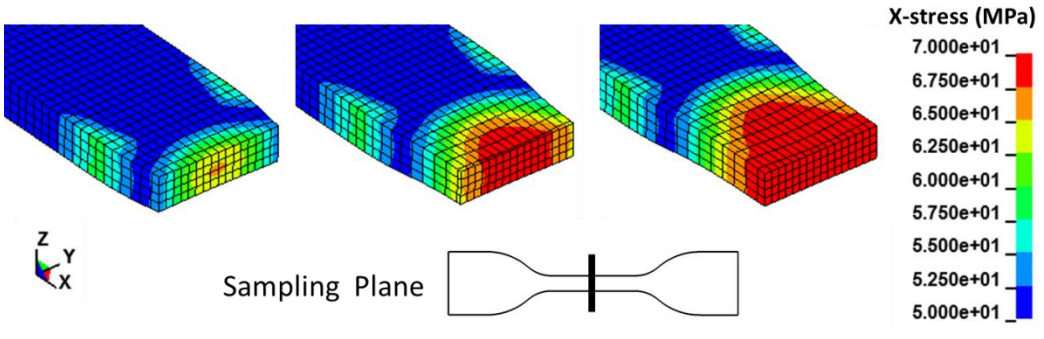


Figure 12: X-stress plot on the cross section of the specimen during necking deformation.

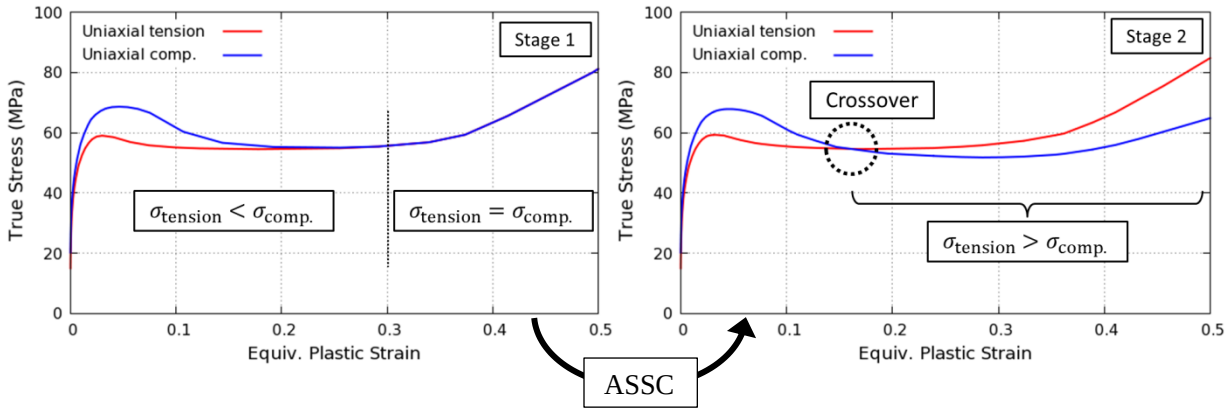


Figure 13: Comparison of SS curves in each stage between uniaxial tension and compression.

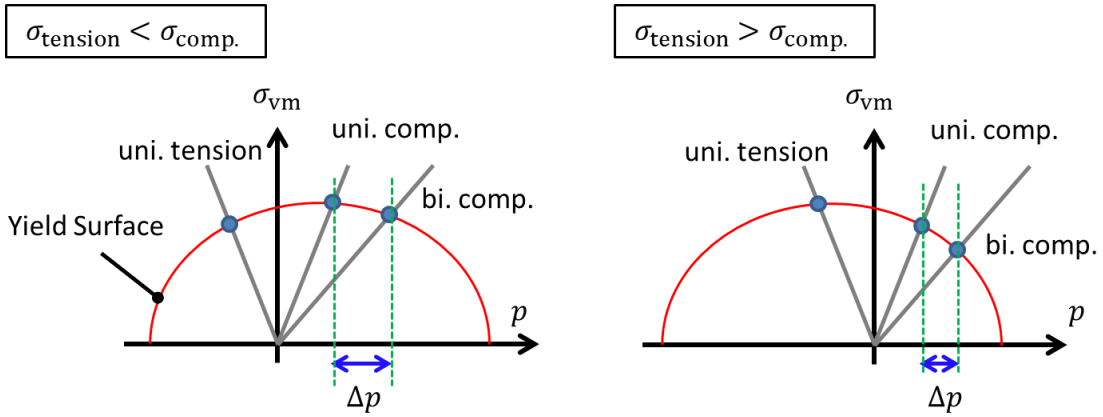


Figure 14: Schematic representation of yield surface in SAMP-1 mode for the polycarbonate.

## Conclusion and Outlook

We have introduced our validation and material modeling method for polymers with MAT_SAMP-1 and have shown examples using polycarbonate through the paper. Though the method in determination of LCID-P and its corresponding SS data seems to be complex, we believe this method is the most effective because it is based on the elasto-plastic algorithm used in MAT_SAMP-1. In addition, our techniques in designing the yield surface have been introduced and have been proved to make calculations stable. Another method to fit damage parameter is also mentioned.

In utilizing MLYS mode, we have prepared LCID-B with reverse engineering calculation from the SAMP-1 yield surface instead of with biaxial tension test. Besides, this LCID-B has not been validated with appropriate test analysis where biaxial tension state dominates. It is important to establish the method of the biaxial test for polymers in future.

## References

[1]. S. Kolling, A. Haufe, M. Feucht and P. A. Du Bois: SAMP-1: A Semi-Analytical Model for the Simulation of Polymers, 4th German LS-DYNA Users Conf., A-II-27/57, 2005

[2]. Stefan Hiermaier: Advanced Methods for the Characterization on Highly Non-Linear Materials for Crash Applications, JAPAN LS-DYNA Users Conf., A-2-1/9, 2007

[3]. A. Ratai, S. Kolling, A Haufe, M. Feucht, P. Du Bois: Validation and Verification of Plastics under Multiaxial Loading, LS-DYNA Anwenderforum, D-I-1/10, 2008

[4]. H. Daiyan, F. Grytten, E. Andreassen, O.V. Lyngstad, H. Osnes, R.H. Gaarder and E.L. Hinrichsen: Numerical simulation of low-velocity impact loading of polymeric materials, 7th Euro. LS-DYNA Conf., D-II-02, 2009

[5]. K. Takekoshi and K. Niwa: Impact and fracture analysis of Polycarbonate structural parts using the material law formulation of polymers, JSME 23rd Comp. Mech. Div. Conf., 1307, 2010

[6]. K. Takekoshi and K. Niwa: A study of methods for the characterization of polymeric materials, JSCES16, B-7-1, 2011

[7]. K. Takekoshi and K. Niwa: The evaluating method of plastic Poisson's ratio, JSME 24th Comp. Mech. Div. Conf., 306, 2011

[8]. M. Vogler, S. Kolling, A. Haufe: A Constitutive Model for Plastics with Piecewise Linear Yield Surface and Damage, 6th German LS-DYNA Users Conf., B-II-13/30, 2007

[9]. LS-DYNA® Keyword User's Manual Volume II Ver.971 R6.0.0, Livermore Software Technology Corporation.

[10]. P. A. Du Bois, S. Kolling, M. Feucht, A. Haufe: The Influence of Permanent Volumetric Deformation on the Reduction of the Load Bearing Capability of Plastic Components, 10th Int. LS-DYNA Users Conf., 19-35/42, 2008